

## Demonstration in space of a smart hyperspectral imager for nanosatellites

Esposito M., Conticello S.S., Vercruyssen N., van Dijk C.N., Foglia Manzillo P.,  
Koeleman C.J  
cosine measurement systems  
Oosteinde 36 2361 HE Warmond, The Netherlands;  
+31 71 524 18 42, m.esposito@cosine.nl

Delauré B., Benhadj I., Blommaert J., Livens S.  
VITO  
Boeretang 200, BE-2400 Mol, Belgium;

Jochemsen A., Soukup M.  
Science [&] Technology AS  
Forskningsparken Gaustadalléen 21, 0349 Oslo, Norway

Menenti M., Gorte B., Hosseini Aria E.  
Delft University of Technology, Stevinweg 1, 2628 CN, Delft, The Netherlands

### ABSTRACT

HyperScout is the first smart hyperspectral imager for nanosatellites. It has been launched on the 2nd of February 2018 at 8:51 CET, from the Jiuquan Satellite Launch Center in China. The launch vehicle Long March 2D lifted off on schedule and the satellite was separated from the launch vehicle minutes later. Approximately after 6 hours the first contact was established by GomSpace in Aalborg, Denmark.

HyperScout is based on a long line of development led by cosine. The project to develop, build and launch the first HyperScout was funded by ESA, with support from the Dutch, Belgian and Norwegian national space organizations: Netherlands Space Office, BELSPO and Norsk Romsenter. cosine, as the prime contractor, enlisted the help of consortium partners S&T, TU Delft, VDL and VITO.

The applications for which HyperScout has been conceived for are crop water management, fire hazard monitoring, flood detection, change detection of land use and land coverage and vegetation monitoring. The aim of the demonstration mission is to assess the quality of the data that will be acquired and the consequent suitability for the intended applications. Furthermore, the basic functionalities of the instrument as well as the onboard processing in real time will be demonstrated. The demonstration is divided in three operational blocks, during which HyperScout will be operated to acquire data from invariant sites for vicarious calibration, from application sites to qualify HyperScout for all the applications it has been conceived for, and to perform software experiments to demonstrate the novel approach to overcome the bandwidth limitation on small platforms.

This paper reports about the outcome of the operations performed so far in orbit, and about the preliminary results obtained from the data evaluation performed during the demonstration project.

### INTRODUCTION

HyperScout® is a miniaturized hyperspectral imager based on a three mirror anastigmat telescope (TMA) and onboard processing units [1]. The extremely compact reflective telescope ensures high optical quality over the entire range of optical wavelengths. The operational onboard data handling system is designed for realtime data processing, enabling Level-2 generation onboard and therefore drastically reducing the amount of data to be downloaded and processed on ground [2]. This mission will benchmark the payload in flight performance and will demonstrate its functionalities.

HyperScout® was launched on the 2nd February 2018 as part of the GomSpace GOMX-4B, ESA's most

advanced CubeSat, on a Long March 2D launch vehicle from JSLC (Jiuquan Satellite Launch Center), China. Besides HyperScout®, the CubeSat carries onboard a number of experimental payloads [5]. During the Launch and Early Operations Phase (LEOP) HyperScout® performed its first functional tests including the acquisition of the first 2 images.

The project was performed under ESA (European Space Agency) GSTP (General Support Technology Programme) contract, by a consortium lead by cosine measurement systems B.V. (NL), including VDL (NL), TUDelft (NL), VITO NV (BE) and S[&]T AS (NO).

## HYPERSCOOUT OVERVIEW

The strength of Hyper Scout® lies in the compact design, low power consumption, low mass and on-board processing capabilities.

HyperScout® is equipped with a 2D sensor and a spectral filtering element to separate the different wavelengths. The On-Board Data Handling system (OBDH) is able to process in real time the acquired L0 data performing geometric corrections and orthorectification allowing the L2 data processing algorithms to analyse the data for a variety of applications. The same data can be processed for all the different identified applications, for example for vegetation conditions and change detection. The objective is to enable the direct download of the processed geophysical data products with coordinate information and to enable early warning [2].

Although HyperScout® is conceived as a CubeSat payload, it can be installed on a large variety of platforms. HyperScout® occupies a volume of about 1.5 CubeSat units [U or dm3], has a mass of 1.3 kg and has a power consumption of 9 W (peak). Thanks to its small engineering budgets and its easily adaptable mechanical interfaces, it can be adapted for integration to any platform [3].

The telescope is an athermal system based on a monolithic structure. The FPA is based on CMOS sensor and a spectral filtering element used to separate the different wavelengths. The ICU is the S/C contact point for the HyperScout® allowing in-flight debugging of the BEE/OBDH subsystem. It is possible to completely power down each subsystem from the ICU.

The BEE is the electrical interface to the spacecraft and is latch-up protected. It distributes power, clocks, telemetry and commands between the units, controls the detector and serves as the data and control interface, providing clock timings, frame rate control, exposure and gain control. The OBDH then merges the data acquired with the platform ancillary information creating L0 data, which is then stored in the payload Mass Memory Unit (MMU).

The OBDH hardware serves multiple purposes, the most distinct being the platform for both the acquisition and the processing modes. During the acquisition mode, data will be transferred from the BEE into the memory of the OBDH, which is then written to the MMU via SATA. During processing mode (L0 to L2A-L2B), the data is retrieved from the MMU and processed in memory on the OBDH.

Both the acquired L0 image data and processed data are stored on board the payload's MMUs. Two MMUs are operated in a hot and cold redundant configuration. The specification of the payload during its in orbit demonstration mission is reported in TABLE 1.

**Table 1: HyperScout®-1 specifications summary for the IOD mission**

Parameter	Value
IOD Orbit	Sun Synchronous, 500 km altitude, LTDN 15:00 hrs
Field of view	23° (ACT) x 16° (ALT) - nominal FOV 31° (ACT) <sup>1</sup>
Ground Sampling Distance	70 m @ 500 km
Swath IOD	200 x 150 km (ACT x ALT) @ 500 km
Spectral range	400 - 1000 nm
Spectral resolution	15 nm
Dynamic range	12 bit
SNR	50-100 @ 500 km
Mass	1.3 kg

<sup>1</sup> The nominal FOV ACT of HyperScout is 31°. However, due to mechanical constraints for the current mission it was reduced to 23°



**Figure 1: HyperScout Flight Model**

**HyperScout® acquisition strategy**

The wavelength separation is performed in the along track direction, with a constant wavelength in the across track direction. The 2D sensor is used in pushbroom mode: the full hyperspectral datacube acquisition requires the acquisition of a series of subsequent frames, so that each region on ground is imaged in all wavelengths and can then be used to reconstruct the hyperspectral datacube. The acquisition sequence is depicted in Figure 2.

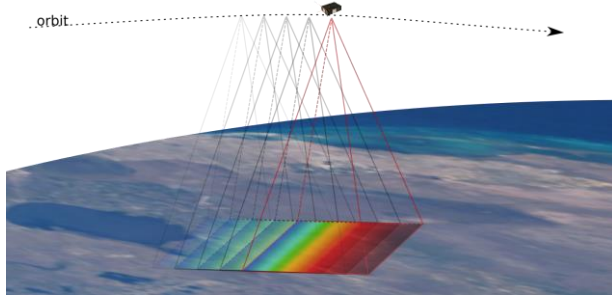


**Figure 2: HyperScout® acquisition sequence**

**HYPERSCOOUT® IOD MISSION OVERVIEW**

At the orbital height of 500 km, HyperScout® will orbit the Earth 15 times a day, with a complete revisit at the equator around 45 days. The satellite will be configured once per day defining the key application for each site and the region of interest.



**Figure 3: Coverage simulation of 8 days**

The HyperScout® operational phase is planned to be completed by the end of 2018. The mission operations are subdivided into blocks, to spread the operations over the nominal mission and monitor the performance of the payload after a long exposure to the space environment. This will also serve the purpose of acquiring data over the same regions of interest at different time intervals to observe seasonal variations.

The first operational block is dedicated to the radiometric calibration, line of sight model correction and instrument functionality testing. During the second operational block of intensive observations L2 data validation will be performed, and in the last block, on board processing experiments will take place.

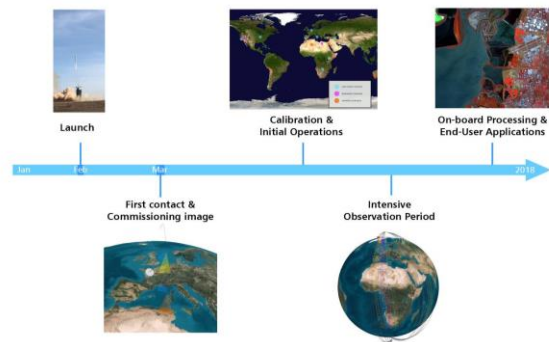


**Figure 4: HyperScout® mission outline**

The IOD mission regions of interest have been identified by the consortium partners and are listed in Figure 5. The regions are both calibration and data product validation targets. During the intensive observation period the data will be compared with Copernicus data, in-situ ground truth measurements and an airborne campaign.

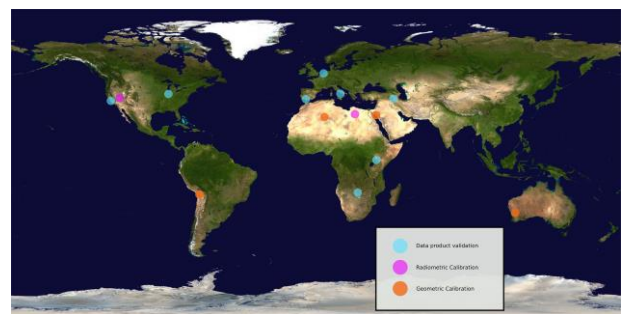


**Figure 5: HyperScout® mission regions of interest**

**HYPERSCOOUT APPLICATIONS**

HyperScout® is a cost-constrained compact imager developed to serve a large variety of applications, among which monitoring of natural disasters such as floods delineation, forest fires hazard and desertification. High revisit times globally (sub-daily) can be achieved with the deployment of a constellation composed of tens of units.

Considering urban areas, materials such as concrete, asphalt, metal roofs, could be classified; in the field of vegetation, recent studies focused on compositional variation of different plant species to extract major vegetation gradients; in the case of wetlands, detection

and monitoring of floods enables a more rapid response to flood risks and assessment of damaged areas. The same applies for fire hazard.

The HyperScout® applications exhibit a worldwide relevance and some of the applications rely on spectral indices as proxy, as are described in the following paragraphs.

### ***Monitoring of vegetation conditions (drought)***

Unlike other forms of severe weather or natural disasters, droughts often develop slowly and their effects vary from region to region. Hence the early detection plays an important role in the mitigation process. The Normalized Difference Vegetation Index (NDVI) provides generic information related to the presence and concentration of chlorophyll in plant leaves. The vegetation index has been considered by numerous scientists as one of the important parameters for the mapping of agricultural fields, estimating weather impacts, calculating biomass, crop yield, drought conditions and determining the vigor of the vegetation.

### ***Crop water requirements***

The crop water requirement (CWR) is defined as the amount of water needed by the various crops to balance the water loss through evapotranspiration, necessary for an optimal plant growth. NDVI is a reliable indicator of crop phenology and as such of leaf display. The latter leads to a correlation with maximum plant transpiration under optimal water supply. Estimation of crop water requirements (CWR) is based on the correlation between the NDVI and the crop coefficient ( $K_c$ ). HyperScout® can generate  $K_c$  values which can be then used to calculate CWR for any determined area of interest.

### ***Fire hazard***

Observations of spectral reflectance are widely used as an indicator of foliage (fuel) conditions and can be used as a forest fire hazard indicator. HyperScout® can acquire and process data over large forest areas which would be otherwise difficult to monitor with traditional methods. For this application the issue of early warnings is essential and is enabled by the real time processing and the short data timeliness.

### ***Delineation of flooded areas***

The Normalized Difference Water Index (NDWI) provides information directly related to the presence of water within a heterogeneous scene including vegetation, soil and built-up areas. Specifically, the

water land boundary line over land can be clearly delineated. Open water areas are identified and subtracted, highlighting the flooded areas. This application can be used to define the floodplain hydraulic model of a particular region of interest, providing a great insight into the response and the behaviour of the region under analysis.

### ***Land cover and land use – change detection***

Land cover and land use - change detection algorithms have been implemented for onboard processing. HyperScout® will create an on-board database of the regions of interest (ROIs) divided in classifiers in which each specific spectral signature feature is recorded. In order to do so, the ROIs need to be observed at all wavelengths (400-1000 nm). Onboard processing aims at detecting spectral changes in the various segments. When this occurs, data is downlinked indicating the detected spectral features change and location. This data product satisfies a number of applications and it can be applied to multiple scenarios, as for example:

- Identification of illegal waste dumping sites and assessment the degree of environmental contamination;
- Monitoring of water quality, identifying algae concentration and suspended contaminants. A major global ecological problem is the increasing eutrophication and pollution of coastal and inland water bodies caused by fluvially transported substances such as phosphate and nitrogen compounds, which derive from intensified agricultural and industrial activities;
- Monitoring of oceanic phytoplankton is also of high interest since it is responsible for about 50% of the global oxygen production [4];
- Identify and track oil spills both on marine and land areas. Hyperspectral data can also be used to determine the oil type and thickness;
- Monitoring of urban areas development;
- Monitoring of coastal and port areas;
- Monitoring of ice, snow-covered areas and sea ice.

### **FIRST LIGHT AND IN ORBIT DATA**

The HyperScout® commissioning was performed following the GOMX-4B satellite main subsystems commissioning. The HyperScout® commissioning

phase aimed at validating the payload functionality chain, from acquisition to compression and downlink to the ground, and assesses the status after launch and after the first weeks of space environment exposure. The payload is therefore powered ON, communication established with the S/C subsystems and a single frame is acquired. The operations sequence for the first commissioning image is depicted in Figure 6. During the orbit 704 HyperScout is configured for the acquisition, during orbit 705 the actual acquisition takes place. Data are downloaded during subsequent contacts with the ground station.

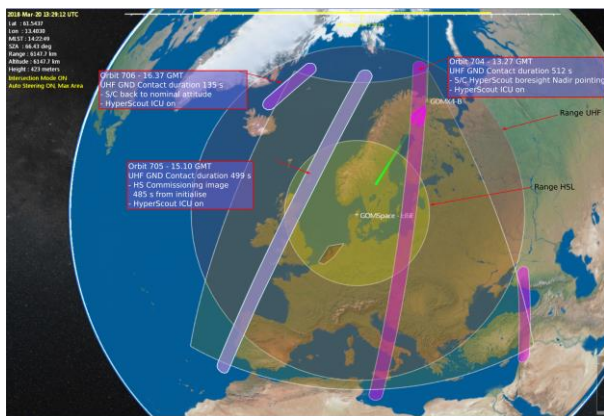


**Figure 6: HyperScout® operations for the acquisition of the first commissioning image.**

Being a single image, each horizontal line shows the scene at a different spectral band. The first light image has been software binned 2x2 and compressed in order to fit within the 1.5 MB allowed data volume requirement dictated by the satellite resources available during the commissioning phase. The image is rendered with false colours based on raw data, therefore the expected effects due to the spectral filtering, the presence of the atmosphere and the solar spectrum are visible as variation of the response along track. This effects will be later calibrated as part of the processing chain. The imaged region is selected randomly based on weather conditions. The first light of the HyperScout® was taken over Scotland and is presented in Figure 7.



**Figure 7: First light of HyperScout. False colour single image of the Scottish landscape between Glasgow and Edinburgh. Image acquired on the 20th of March 2018**

During the first commissioning image acquisition a race condition in setting the region of interest on the sensor

prevented acquiring a full frame. This resulted in cropping the image on the sensor covering only the 400-600 nm spectral bands. This issue was swiftly identified and fixed in order to acquire a second commissioning image, which resulted the full frame image over Cuba, shown in Figure 10.

The frames acquired are binned and have not been calibrated, however a first check on the response shows consistency with typical responses over water. The red curve in Figure 8 shows the typical water response, while Figure 12 shows the relative response of HyperScout.

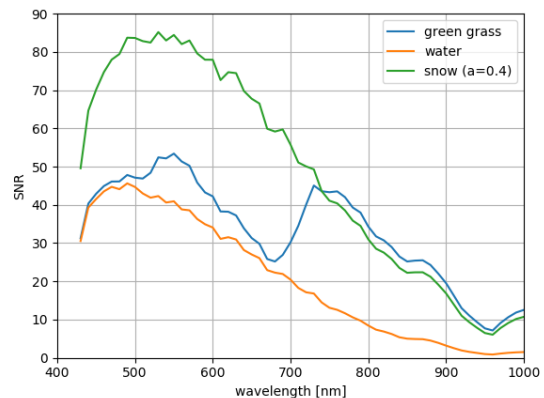


**Figure 8: Typical response of green grass, water and snow.**

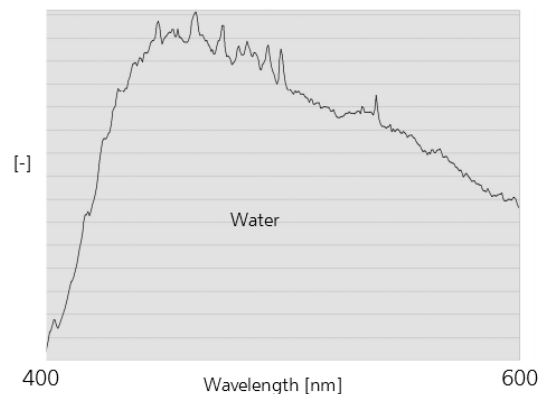


**Figure 9: HyperScout response over water retrieved from the first commissioning image.**

In both images, the amount of light captured by HyperScout® is exceeding expectations, therefore the achievable SNR is very promising enabling many hyperspectral applications.

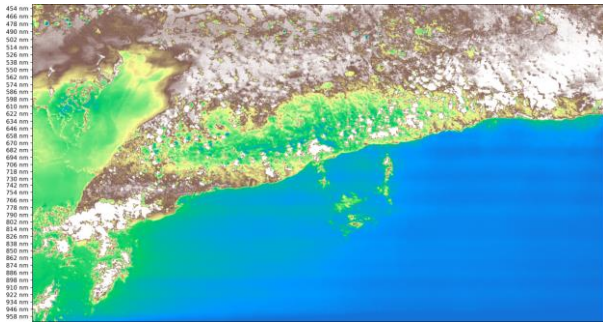


**Figure 10: Commissioning image of HyperScout®. False colour single image of the southern Cuban coastline. Image acquired on the 26th of March 2018**

Together with the image, the HyperScout® housekeeping data was downlinked. All the systems logs are nominal while the subsystems temperatures are presented in Figure 11.

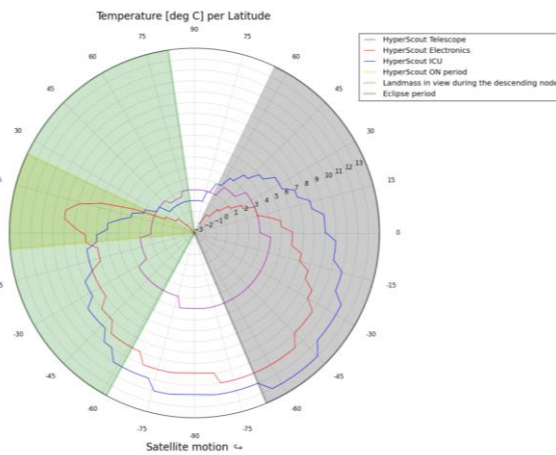


**Figure 11: HyperScout® subsystems temperature plot relative to the revolution of the Cuba acquisition**

The polar plot in Figure 12 describes the temperature of three main subsystems, the HyperScout® telescope, the ICU and the BEE. The log starts and ends with the spacecraft out of eclipse, indicated by the grey area. HyperScout® is equipped with an athermal telescope thermally isolated from the platform by design, and the measured temperature data is stable within 2.5°C over the section of the daylight revolution covering the landmass. The other subsystems do not experience a large temperature variation, considering that they include electronics units that are turned ON for a limited time period.

Characterisation of the telescope at different temperatures was performed prior to launch at the cosine facilities and it did not show any noticeable change in performance. Such a low temperature

variation contributes to a stable line of sight model of the instrument throughout the operational phase of the orbit. During the acquisition of a hyperspectral data cube (~40 s duration) the temperature of the system is expected to be well within 1°C. A more graphical representation of the telescope temperature variation during the course of the second commissioning revolution is presented in Figure 12.



**Figure 12: HyperScout® telescope temperature variations through out the commissioning orbit.**

## CONCLUSIONS

The initial stages of the HyperScout® in orbit demonstration mission are so far a success. The core subsystems have been demonstrated to be operational, the telescope optical performance did not degrade during the launch and two commissioning images were taken, demonstrating a light collection efficiency above expectations and a stable temperature of the optics.

The calibration is the ongoing phase and then will be followed by the operational phase in which the full payload capabilities will be proven.

## ACKNOWLEDGMENTS

The authors wish to acknowledge: Luca Maresi and Alessandro Zuccaro Marchi of ESA ESTEC TEC/MMO, for their valuable support and commitment that made possible to build the HyperScout® Flight Model; Mathieu Breukers of VDL ETG Research B.V. for the manufacturing of the HyperScout optics; The Netherland Space Office (NSO), the Belgian Science Policy Office (BELSPO) and the Norwegian Space Centre (NSC) for funding the project through the ESA GSTP program..

## REFERENCES

1. Simon Silvio Conticello, Marco Esposito, Pierluigi Foglia Manzillo, Chris Van Dijk, Nathan Vercruyssen, Pieter-Jan Baeck, Iskander Benhadj, Stefan Livens, Bavo Delaure, Michael Soukup, Arnoud Jochemsen, Christina Aas, Ben

- Gorte, Enayat Hosseini Aria, Massimo Menenti, Hyperspectral imaging for real time land and vegetation inspection, 4S Symposium, 2016
2. Michael Soukup, Janis Gailis, Daniele Fantin, Arnoud Jochemsen, Christina Aas, Pieter-Jan Baeck, Iskander Benhadj, Stefan Livens, Bavo Delauré, Massimo Menenti, Ben Gorte, Seyed Enayat Hosseini Aria, Marco Esposito, Chris van Dijk, 4S Symposium, 2016
  3. Ivan Ferrario, Massimiliano Rossi, Fabio E. Zocchi, Giovanni Bianucci, Marco Esposito, Simon Silvio Conticello, Hyperstreego: Reactive payload, 4S Symposium, 2016
  4. Oxygen Factories in the Southern Ocean, 13 January 2016, NASA Visible Earth , retrieved from <https://visibleearth.nasa.gov/view.php?id=87465>, accessed in April 2018.
  5. [http://www.esa.int/Our\\_Activities/Space\\_Engineering\\_Technology/The\\_size\\_of\\_a\\_cereal\\_box\\_ESA\\_s\\_first\\_satellite\\_of\\_2018](http://www.esa.int/Our_Activities/Space_Engineering_Technology/The_size_of_a_cereal_box_ESA_s_first_satellite_of_2018)